

Degradation Behavior of Nanostructured Coatings Deposited by High-Velocity Arc Spraying Process in an Actual Environment of a Coal-Fired Boiler

V.N. SHUKLA,¹ R. JAYAGANTHAN,^{1,2} and V.K. TEWARI¹

1.—Department of Metallurgical and Materials Engineering & Centre of Nanotechnology, Indian Institute of Technology Roorkee, Roorkee 247667, India. 2.—e-mail: rjayafmt@iitr.ernet.in

FeCr-based nanostructured coatings were deposited on a 301S stainless steel substrate by the high-velocity arc spraying process in the current work. The oxidation behavior of the coatings exposed to elevated temperatures (700°C and 900°C) under laboratory conditions as well as in an actual industrial environment of a coal-fired boiler (at $700 \pm 10^\circ\text{C}$) was investigated. X-ray diffraction, scanning electron microscopy/energy-dispersive analysis, and transmission electron microscopy techniques were used to characterize the coating as well as to analyze the corrosion products for elucidating the corrosion mechanisms. The microhardness of the coating was found to be 520–1100 HV. The (FeCr)-based nanostructured coating showed good adherence to the 310S substrate and excellent oxidation resistance during the exposures with no tendency for spallation of its oxide scales in both environments. The nanosized grain morphology of the coating facilitated the formation of protective scales, which is continuous, adherent, and nonporous due to the higher diffusivity of alloying elements in the coatings. It precludes high-temperature oxidation by acting as a diffusion barrier between the environment and the coating.

INTRODUCTION

The degradation of metals in high-temperature aggressive environments is a serious problem for boiler tubes of coal-fired boilers.^{1,2} Huge amounts of material wastage in power generation plants due to combustion of fuels are reported.^{3–8} The literature reveals the wide contribution of thermal-sprayed coatings for the safety of boiler tubes against high-temperature corrosion attack.^{9–16}

Thermally sprayed cermets have emerged as a viable solution for providing necessary protection against wear and corrosion. The high-temperature oxidation resistance of Fe based high-chromium and nickel containing alloys is extensively used to fabricate corrosion- and wear-resistant coatings. These Fe-base coatings are deposited by different thermal spray techniques such as plasma spray process, detonation gun process, and high-velocity oxy-fuel process (HVOF). Among all these thermal spray processes, high-velocity arc spraying (HVAS) process is usually employed due to its cost effectiveness

(operating at a lower cost), high deposit efficiency, and fewer applications difficulties.¹⁷ The HVAS process has a capability of producing dense coating with higher bond strength and lower oxide content.¹⁸ Thermally sprayed Fe-base coatings have been used extensively to inhibit/mitigate wear, erosion, and corrosion at elevated temperatures in gas turbines, steam turbine, power generation industry, and coal-burning boiler tubes.^{19–22}

Information on the influence of microstructural features on erosion–corrosion performance in actual coal-fired boiler environment (at $700 \pm 10^\circ\text{C}$) and the oxidation behavior of HVAS nanostructured coatings is limited in the literature. The degradation mechanisms of nanostructured coatings exposed to a high-temperature environment (700°C and 900°C) has not been subjected to detailed study thus far. Knowledge of the reaction kinetics and microstructural changes of the oxide scales formed at high elevated temperatures is important for evaluating the performance of materials in high-temperature applications.^{23,24}

Table I. Chemical composition (wt.%) of a nanostructured wire material

Cr	W	Nb	Mo	B	C	Mn	Si	Fe
<25	<15	<12	<6	<5	<4	<3	<2	Bal.

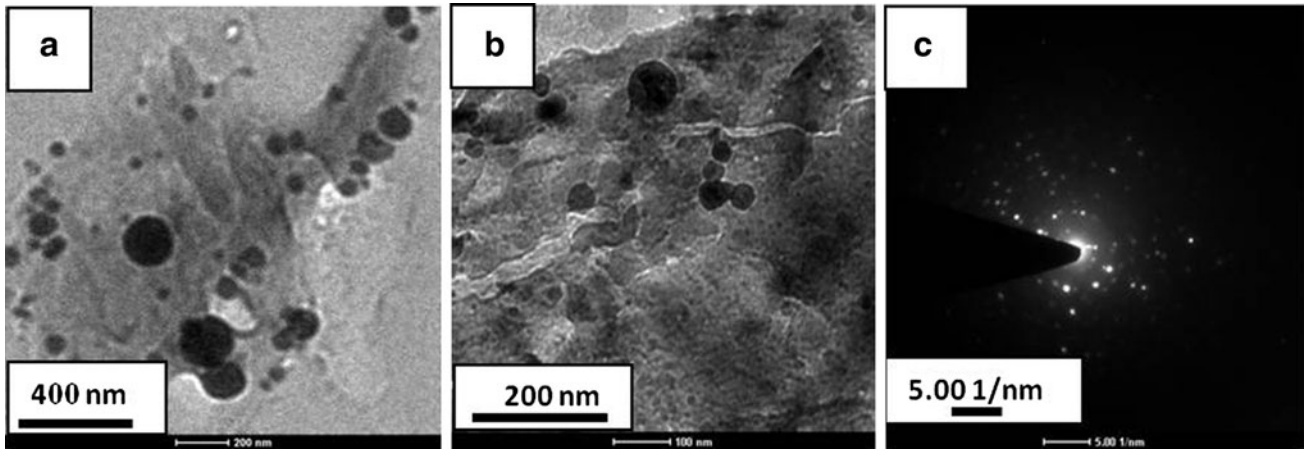


Fig. 1. TEM images of (a) the nanostructured wire material (powder inside the cored wire) and (b) TEM images and (c) SAED pattern of typical microstructure of the as-sprayed coating on 310S substrate.

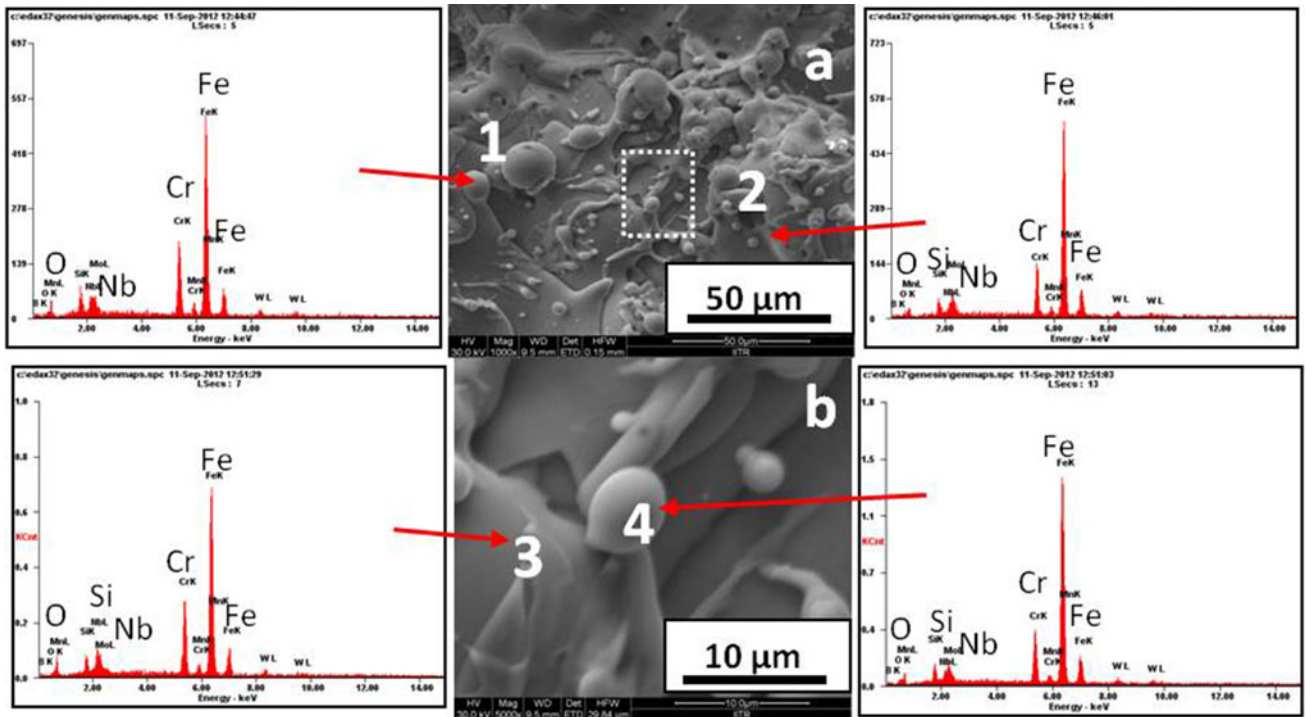


Fig. 2. Fe-SEM/EDS with EDS analysis showing the surface morphology for the as-sprayed coating on a 310S substrate: (a) 50 μm , (b) 10 μm .

Therefore, the current work was focused to study the erosion–corrosion performance of HVAS nanostructured coatings deposited on 310S. The microstructural features and oxidation behavior these

coatings at 700°C and 900°C were investigated by using field-emission scanning electron microscopy/energy-dispersive analysis (FE-SEM/EDS), x-ray diffraction (XRD), and thermogravimetric technique,

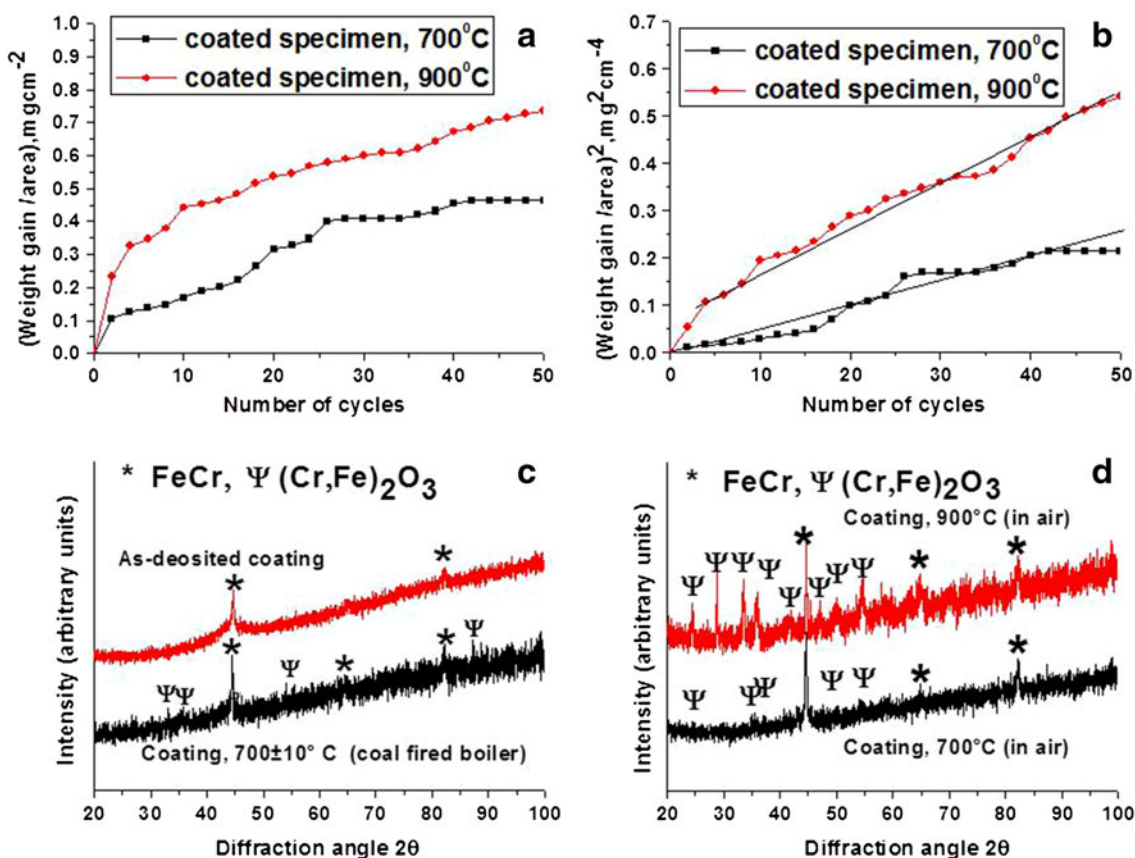


Fig. 3. (a) Weight gain/area versus number of cycles and (b) (weight gain/area)² versus number of cycles plot for the coated specimens, after cyclic oxidation of 50 cycles in air at 700°C and 900°C. The XRD patterns of the scale formed on coated specimen. As-deposited coating and coating subjected to cyclic oxidation in (c) coal-fired boiler at 700 ± 10°C for 1500 h and (d) coated specimens after cyclic oxidation of 50 cycles in air at 700°C and 900°C.

respectively. The variations in microstructural morphology were correlated with the oxidation behavior of bare and coated specimens.

EXPERIMENTAL

310S steel substrate plates were used as substrates. The gauge size of substrates used was 20 mm × 15 mm × 5 mm. Prior to coating, the substrates were degreased using acetone, dried in air, and then grit blasted by alumina (grit 45). Blowing by compressed air was carried out to remove the alumina particles and then HVAS was executed using the standard spray parameters, at M/s Industrial Processors and Metallizers (IPM), Pvt. Ltd. (New Delhi, India). Fe-base cored wires (TAFA 140 MXC; Tafa Incorporated, Concord, NH) were used as feedstock. The chemical composition (wt.%) is listed in Table I.

The microstructures of nanostructured wire material and the coatings were characterized by XRD, transmission electron microscopy (TEM; FEI-Technai-21; FEI Company, Hillsboro, OR) and field-emission scanning electron microscopy (FE-SEM;

Quanta 200 FEG-SEM; FEI Company) with EDAX Genesis software attachment (EDAX Inc., Mahwah, NJ). XRD analysis was carried out using a Bruker AXS D-8 Advance powder diffractometer (Bruker Corporation, Germany) with CuK_α radiation (1.5410 Å). Prior to the corrosion runs, the physical dimensions of the coated specimens were measured with a Sylvac digital vernier caliper (resolution 0.01; Sylvac, Crissier, Switzerland). The microhardness of the as-deposited nanostructured coating on 310S substrate was measured by using Micro Hardness Tester (VHM-002 Walter UHL, Germany) using 300 g (2.941 N) load applied for a dwell time of 15 s. The microhardness of coating was found to be (520–1100 HV).

The cyclic oxidation studies on nanostructured coatings were performed in air at 700°C and 900°C for 50 cycles. One hour heating in a SiC tube furnace, followed by 20 min cooling at room temperature (25°C) was adopted in each cycle. Weight-change measurements were carried out at the end of each cycle with the help of an electronic balance with a sensitivity of 0.1 mg. Any spalled scale during oxidation was also included at the time of

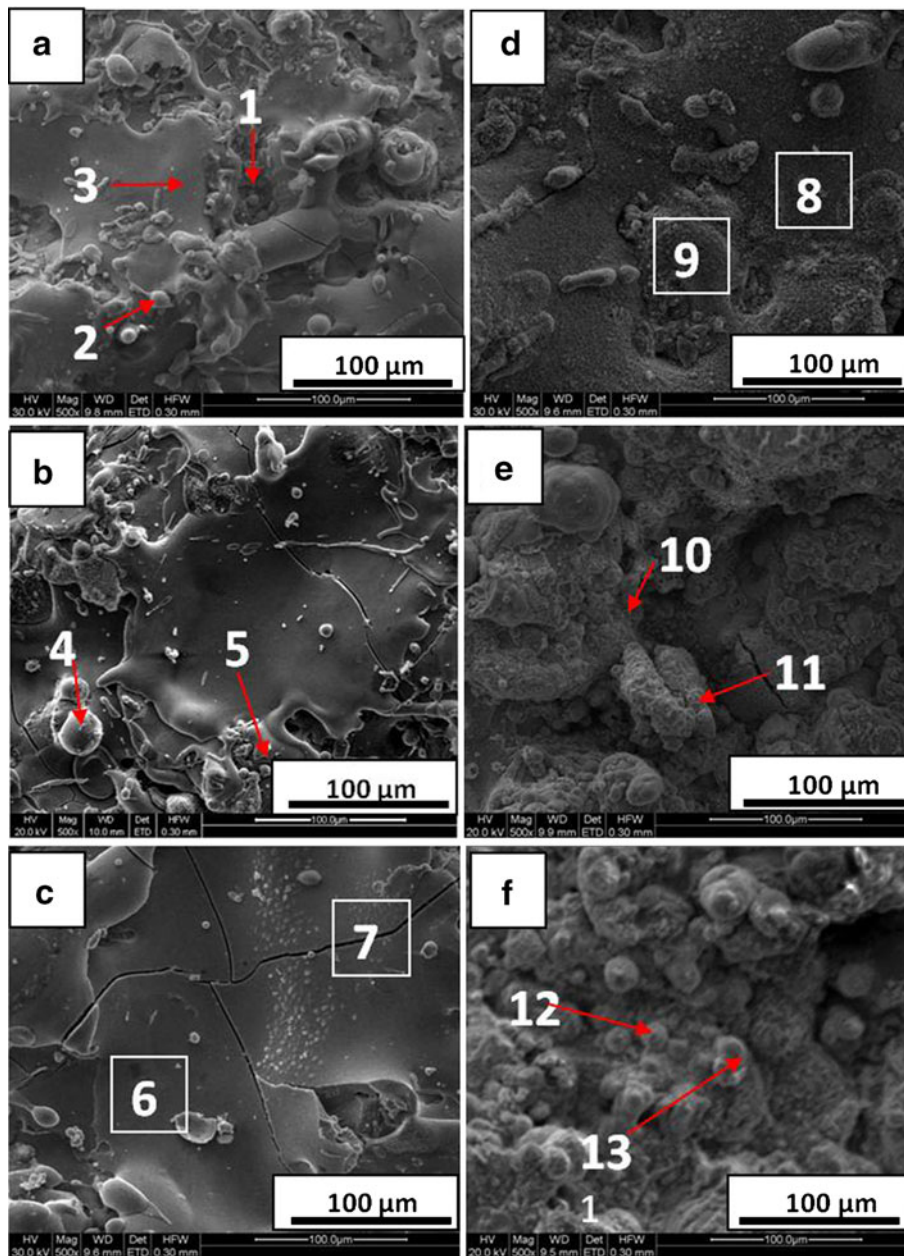


Fig. 4. Fe-SEM/EDS with EDS analysis of coating on 310S substrate showing elemental composition (wt.%) at selected points subjected to cyclic oxidation of 50 cycles in air, at 700°C: (a) after 10 h, (b) after 30 h, (c) after 50 h, and at 900°C: (d) after 10 h, (e) after 30 h, and (f) after 50 h.

weighing to determine the rate of oxidation. The oxidation kinetics of the nanostructured coating was substantiated.

Erosion–corrosion studies on coated specimen were performed in a stage II boiler of the Guru Gobind Singh Super Thermal Power Plant (Roop Nagar, Punjab, India). The cyclic studies were performed on the coated specimen in the super heater zone of a coal-fired boiler (at $700 \pm 10^\circ\text{C}$). The specimens were hanged in boiler (at stage II) $700 \pm 10^\circ\text{C}$ for 1500 g. The methodology for oxidation testing and characterization can be found

elsewhere.²⁵ The scale of corroded specimen was analyzed by FE-SEM/EDAX and XRD.

RESULTS AND DISCUSSION

Powder and Coating Characteristics

The morphology of the nanostructured wire material and as-sprayed coatings was investigated by TEM and FE-SEM. Figure 1a shows the TEM images of the nanostructured wire material, which confirms the nanometric size of the initial spherical powder particles. The size of nanostructured wire

Table II. EDS analysis results (wt.%) corresponding to Fig. 4 for the coated specimen subjected to cyclic oxidation in air at 700°C and 900°C

Points	B	C	O	Si	Cr	Mn	Fe	Nb
1	0	0	4.34	3.4	17	1.59	60.62	13.05
2	0	0	2.37	3.3	17.02	0.85	63.86	12.6
3	0	1.81	4.64	5.69	15.92	1.02	55.2	15.5
4	5.13	0.77	3.44	0.56	6.68	0.42	22.06	56.63
5	0	1.13	21.40	0.51	12.14	0.62	28.10	31.23
6	0	0	7.76	4.30	20.47	1.44	57.55	8.76
7	0	0	6.20	3.17	19.57	0.68	64.53	5.85
8	0	4.85	20.25	20.51	11.59	1.72	37.68	3.39
9	0	0	8.19	1.28	22.12	2.18	61.51	3.60
10	1.17	0.75	11.77	0.59	8.67	0.88	13.70	62.41
11	0.82	1.11	7.67	0.35	3.72	1.01	17.33	64
12	0	4.22	26.39	2.01	26.26	1.44	36.83	1.24
13	0	2.32	17.89	3.12	29.37	2.10	43.04	1.51

materials used for coating was found to be in the range 10–120 nm. TEM image shown in Fig. 1b indicates the presence of nanocrystalline particles in the coating. Figure 1c shows the concentric bright rings in the SAED pattern, which indicates the polycrystalline nature of nanostructured particles in the coating.²¹

FE-SEM images of the nanostructured coating are shown in Fig. 2a, b. The microstructures revealed that high-velocity arc sprayed nanostructured coating is dense, smooth, and without any microcracking.²¹ The coating surface was free of loose particles. Also, the coating surface consisted of the globules of sprayed splats. An EDS analysis (see insets in Fig. 2a, b) of the coating surface indicates the presence of Fe and Cr as major elements and Si, Nb, O, W, and B as minor elements. The microhardness of coating was found to be (520–1100 HV). It is high due to the dense structure of the coatings consisting of nanosized particles.

Figure 3c shows the XRD pattern of the as-sprayed nanostructured coating. The characteristic diffraction peaks of FeCr phase are present in the as-sprayed coating surface. The absence of any other oxides reveals strong resistance to oxidation of the coating in ambient conditions. The average crystallite size for the as-sprayed nanostructured coating was found to be 34 nm, which was calculated by using the Debye-Scherrer formula.

Thermogravimetric Analysis

Weight change per unit area (mg/cm^2) versus the number of cycles plots for the coated specimen subjected to cyclic oxidation at 700°C and 900°C in air up to 50 cycles is shown in Fig. 3a. The plot reveals that coated specimens have undergone lesser overall weight gain at 700°C as compared to at 900°C. It is obvious from the plots that at 700°C, the coated specimen shows a general tendency to approach a steady state after a gradual increase in weight during the initial 26 cycles of the study. However, a high rate

of increase in weight gain was observed with some spalling at high temperature (900°C), up to 50 cycles of the study. It should be noted that in spite of the macrocracks observed on the surface of the coated specimen after exposure at 700°C for 50 h (see Fig. 4c), the weight gain did not increase rapidly. This suggests superior resistance of high-temperature oxidation of the nanostructured (FeCr)-based coating. In Fig. 3b, the square of weight gain per unit area (mg^2/cm^4) versus the number of cycles for coated and uncoated specimens is plotted. The trend in oxide growth at 700°C and 900°C can be approximated to a parabolic relationship. The parabolic rate constants K_p values for the coated specimen subjected to cyclic oxidation in air for 50 h at 700°C and 900°C were calculated and found to be $1.39 \times 10^{-12} \text{ g}^2 \text{ cm}^{-4} \text{ s}^{-1}$ and $2.69 \times 10^{-12} \text{ g}^2 \text{ cm}^{-4} \text{ s}^{-1}$, respectively. The K_p value for the coated specimen at 700°C was found to be nearly one half of the K_p value of the coated specimen at 900°C.

Surface Analysis of Oxidized Specimens

A detailed analysis of surfaces of coated specimens after oxidization at 700°C and 900°C for 10, 30, and 50 cycles is shown in Fig. 4a–f. An FE-SEM analysis of the coated surface at 700°C indicates loosely bound oxide particles after 10 cycles of oxidation (Fig. 4a), while the thick layers of oxides are found after oxidation at 30 and 50 cycles (Fig. 4b, c). An EDS analysis listed in Table II indicates the major presence of Cr, O, and Fe along with minor presence of Nb, C, Mn, and Si. The cracks observed after oxidation for 30 and 50 cycles indicate spalling of the oxide scales (Fig. 4b, c).

The surface of the oxidized coated specimen at 900°C shows the spongy nodules after oxidation for 10 cycles (Fig. 4d). An EDS analysis of nodules indicates Cr, O, and Fe. A minor amount of Nb, Si, and Mn is detected in the oxide scale. With an increase in the number of cycles to 30, the number of nodules increased. The presence of cracks can

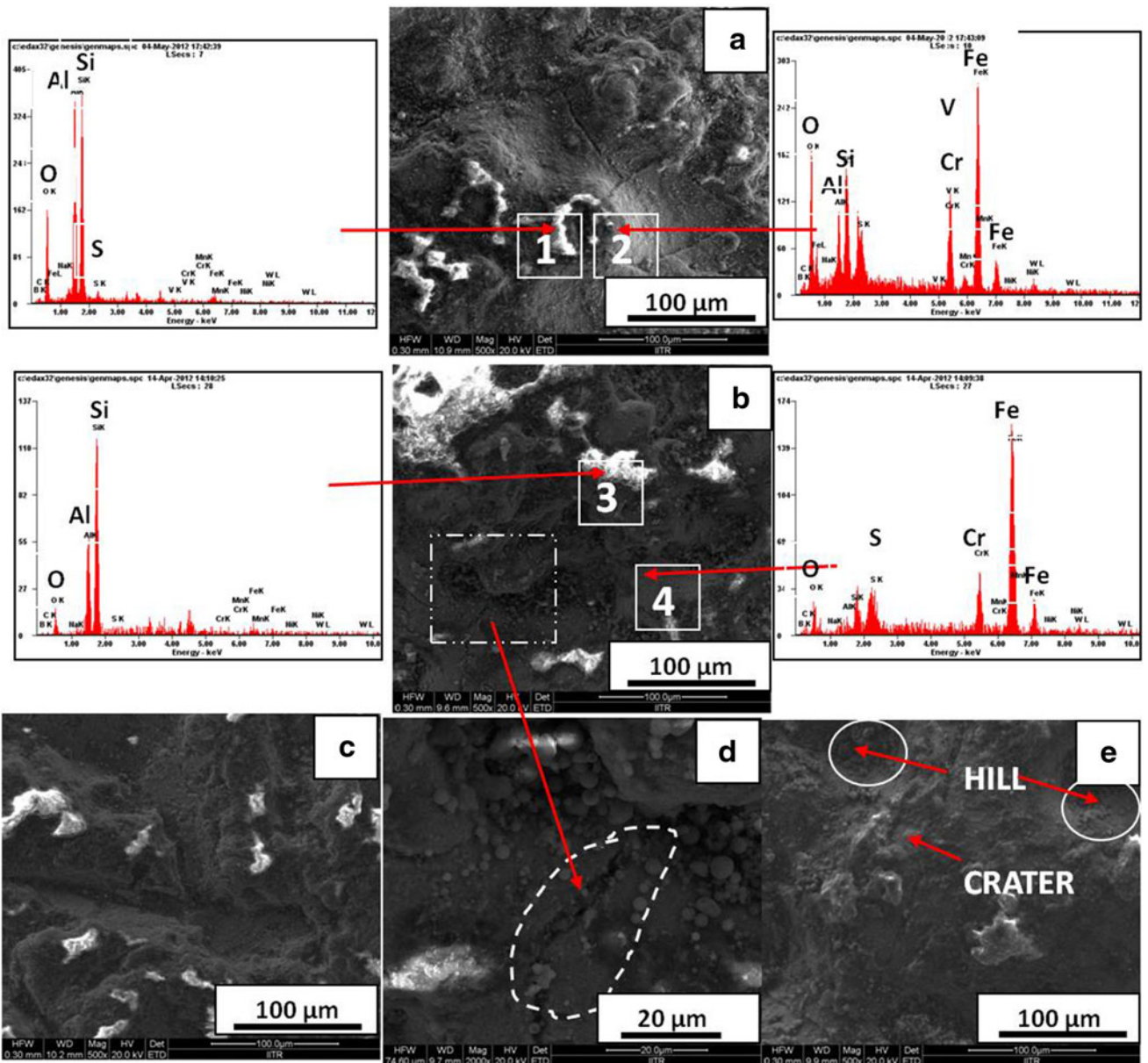


Fig. 5. Fe-SEM/EDS with EDS analysis of coating on a 310S substrate showing elemental composition (wt.%) at selected points subjected to cyclic oxidation in coal-fired boiler at $700 \pm 10^\circ\text{C}$ for 1500 h.

Table III. EDS analysis results (wt.%) corresponding to Fig. 5 for the coated specimen subjected to cyclic oxidation in a coal-fired boiler at $700 \pm 10^\circ\text{C}$ for 1500 h

	B	C	O	V	Al	Si	S	Cr	Mn	Fe	Ni	W	Nb
1	0	5.0	30.22	0.41	20.33	23.32	1.28	0.21	0	3	0.17	0.97	14.54
2	4.64	1.68	7.75	0.23	0.39	1.25	0.77	10.67	0.34	12.94	0.21	4.06	54.91
3	0	0	13.13	0	24.74	54.21	0	0.93	0	6.99	0	0	0
4	1.08	1.76	3.08	0	0.13	0.57	0.62	3.51	0.44	17.96	0.39	3.15	67.26

also be observed on the surfaces after 10 and 30 cycles (Fig. 4d, e). However, the surface is completely covered by the nodules after oxidation for 50 cycles (Fig. 4f). Furthermore, an EDS analysis of

the nodules shows the major presence of Fe, Cr, and O. An XRD analysis of the surface of the coated specimen after 50 cycles at 700°C and 900°C revealed the presence of $(\text{Cr,Fe})_2\text{O}_3$ (Fig. 3d).

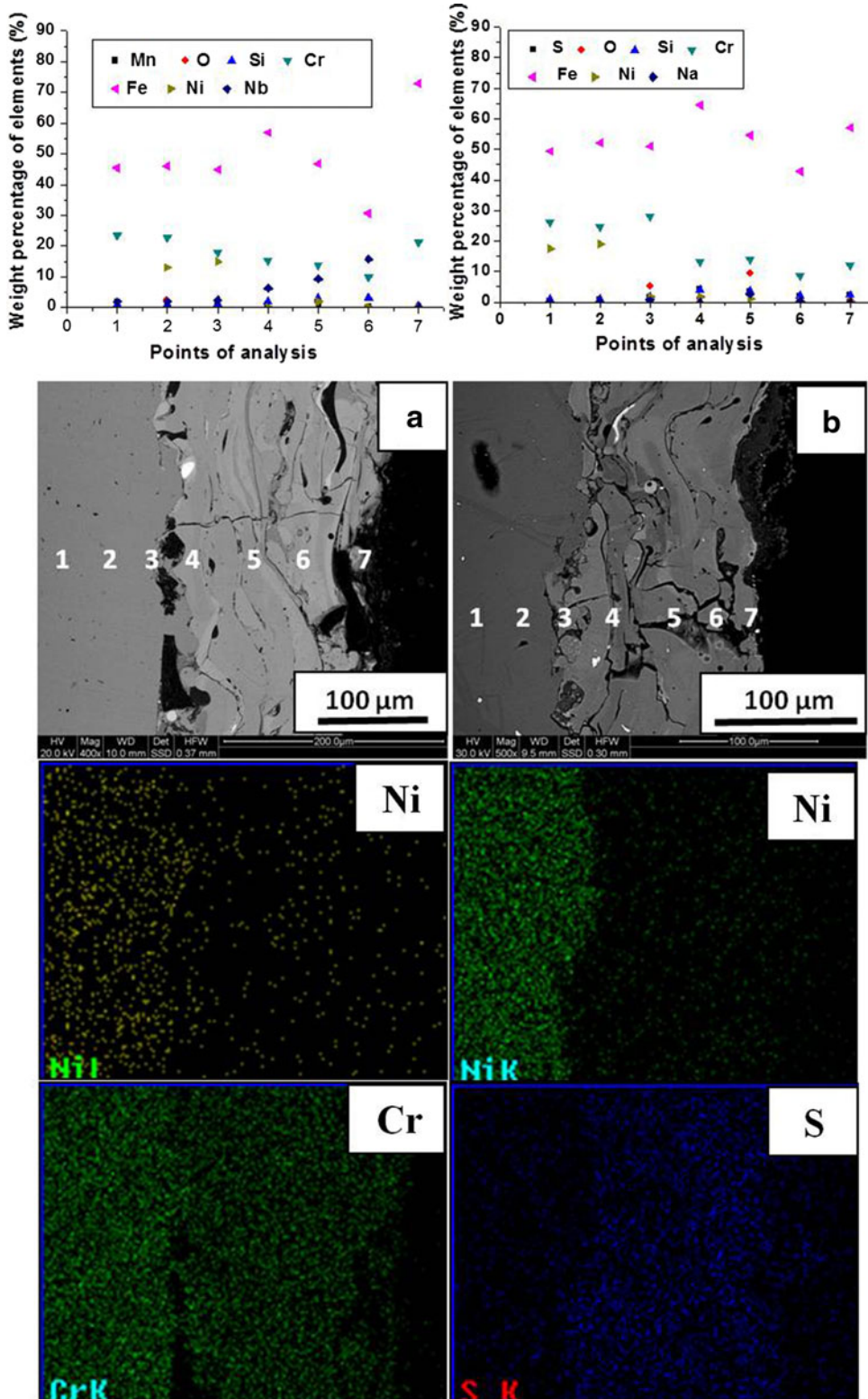


Fig. 6. Morphology of oxide scale and x-ray mapping of the cross section of coated specimen (a) subjected to cyclic oxidation in air at 900°C for 50 cycles, and (b) subjected to cyclic oxidation in coal-fired boiler at 700 ± 10°C for 1500 h.

To assess the performance of nanostructured FeCr-based coating in the actual service conditions, the coated specimens were placed in the industrial

coal-fired boiler for 1500 h at 700 ± 10°C where fly ash particles are continuously thrown on the specimen. The results indicate that the coatings

deposited on 310S steel by the HVAS process do not degrade in the boiler environment. An FE-SEM analysis of the coated specimen after 1500 h of exposure in the boiler environment is shown in Fig. 5. The oxide scale was adherent and minor spalling was observed at the edges of the coated specimen. The surface also shows the pull-out of nodules (Fig. 1). The periphery of the pulled-out areas indicates white contrast, the EDS analysis of which confirms the fly ash elements Al, Si, and O. This indicates that the high-velocity fly ash particles erode the oxide surface of the coated specimen. Furthermore, the long and wider ploughs, craters, and rough areas on the surface are signatures of erosion caused by the fly ash particles (Fig. 5c–e). The scale consisted mainly of Cr, Fe, and O, with significant amount of Al, Si, Mn, and Na. The presence of ash deposited on the surface of coating was confirmed by EDS analysis (Table III). The oxide scale formed on the surface of coated specimen subjected to cyclic oxidation in coal-fired boiler at $700 \pm 10^\circ\text{C}$ for 1500 h was partially removed due to particle impact. An XRD analysis of the oxidized surface of the coated specimen after 1500 h of exposure, in a coal-fired boiler environment, shows the presence of FeCr, $(\text{Cr,Fe})_2\text{O}_3$ phases. A rough estimate of the thickness loss and its rate of loss for HVAS coatings were found to be 0.04 mm and 9.2 mpy, respectively. The weight gain per unit area for the HVAS coating was found to be 7.81 mg cm^{-2} . This small weight gain in case of coated specimen can be attributed to the oxidation and deposition of ash particles on exposed surfaces.

The cross-sectional analysis of the coated specimens subjected to cyclic oxidation in air at 900°C after 50 cycles is shown in Fig. 6a. The similar analysis of coatings subjected to cyclic oxidation in a coal-fired boiler at $700 \pm 10^\circ\text{C}$ for 1500 h was performed and shown in Fig. 6b. Figure 6a shows that the scale mainly consists of oxides of Fe and Cr along with significant amounts of Ni. The oxide scale is found to be continuous, dense, and adherent. Figure 6b shows the scale mainly consists of oxides of Cr and Fe. X-ray mapping of different elements is shown in Fig. 6. The oxide scale is dense and uniform in thickness. However, in the case of a coal-fired boiler, the scale mainly consists of oxides of Cr and Fe, whereas S and Na have diffused into the coating. The formation of oxides of chromium and iron might have acted as barrier to the inward diffusion of oxygen into the coating.

CONCLUSIONS

Nanostructured coatings were deposited successfully on 310S by the HVAS process. Nanostructured

as-sprayed coatings exhibited a very smooth and dense morphology. The coating after cyclic oxidation was found to be intact with the substrate as there is no sign of cracks and gaps at the interface. The oxidation behavior of coating was found to obey parabolic rate law. HVAS-coated specimens exhibited excellent oxidation and wear/spallation resistance. The oxide of Fe and Cr is responsible for imparting resistance against high-temperature oxidation on the coated specimen.

ACKNOWLEDGEMENTS

The authors would like to express their thanks to M/s Industrial Processors and Metallizers (IPM), Pvt. Ltd., New Delhi, India for providing the powders and coating facilities.

REFERENCES

1. T.S. Sidhu, S. Prakash, and R.D. Agrawal, *Surf. Coat. Technol.* 201, 273 (2006).
2. T.S. Sidhu, S. Prakash, and R.D. Agrawal, *J. Therm. Spray Technol.* 15, 811 (2006).
3. D. Wang, *Surf. Coat. Technol.* 36, 49 (1988).
4. S. Collins, *Power* 137, 51 (1993).
5. B. Wang, *Wear* 199, 24 (1996).
6. S. Kamal, R. Jayaganthan, and S. Prakash, *Surf. Coat. Technol.* 203, 1004 (2009).
7. M. Kaur, H. Singh, and S. Prakash, *J. Therm. Spray Technol.* 18, 619 (2008).
8. J.H. He, M. Ice, M. Schoenung, D.H. Shin, and E.J. Lavernia, *J. Therm. Spray Technol.* 10, 293 (2001).
9. B.S. Sidhu, D. Puri, and S. Prakash, *Mater. Sci. Eng. A* 368, 149 (2004).
10. M.H. Staia, T. Valente, C. Bartuli, D.B. Lewis, C.P. Constable, A. Roman, J. Lesage, D. Chicot, and G. Mesmacque, *Surf. Coat. Technol.* 146–147, 563 (2001).
11. B.S. Sidhu and S. Prakash, *J. Mater. Process. Technol.* 172, 52 (2006).
12. S.S. Chatha, H.S. Sidhu, and B.S. Sidhu, *Surf. Coat. Technol.* 200, 4212 (2012).
13. M. Kaur, H. Singh, and S. Prakash, *Surf. Coat. Technol.* 206, 530 (2011).
14. S. Kamal, R. Jayaganthan, and S. Prakash, *J. Alloy. Compd.* 472, 378 (2009).
15. J.K.N. Murthy and B. Venkataraman, *Surf. Coat. Technol.* 200, 2643 (2006).
16. G. Barbezat, A.R. Nicoll, and A. Sickinger, *Wear* 162–164, 529 (1993).
17. B.Q. Wang and M.W. Seitz, *Wear* 250, 755 (2001).
18. G. Liu, K. Rozniatowski, and K.J. Kurzydowski, *Mater. Charact.* 46, 99 (2001).
19. L.L. Ma, L.S. Gaung, Y. Jia, L. Juan, and L. Jian, *Trans. Nonferrous Met. Soc. China* 20, 201 (2010).
20. V.E. Buchanan, *Surf. Coat. Technol.* 203, 3638 (2009).
21. J. Cheng, X. Liang, B. Xu, and Y. Wu, *J. Non-Cryst. Solids* 355, 1673 (2009).
22. C.A. Schuh, T.C. Hufnagel, and U. Ramamurty, *Acta Mater.* 55, 4067 (2007).
23. S. Matthews, M. Hyland, and B. James, *Acta Mater.* 51, 4267 (2003).
24. N. Hussain, K.A. Shahid, I.H. Khan, and S. Rahman, *J. Oxid. Met.* 41, 251 (1994).
25. V.N. Shukla, R. Jayaganthan, and V.K. Tewari, *Adv. Mater. Res.* 585, 483 (2012).